Simulation Study of Monolithic MoSe 2 /CIGS Tandem Solar Cells

B. Zaidi (beddiaf.zaidi@univ-batna.dz)
University of Batna 1
C. Shekhar
Amity University Gurgaon
B. Hadjoudja
University of Badji-Mokhtar
S. Gagui
University of Badji-Mokhtar
S. Zahra
University of Education
M. A. Saeed
University of Education

Short Report

Keywords: Tandem solar cells, SCAPS-1D, Simulation, MoSe2

Posted Date: June 25th, 2021

DOI: https://doi.org/10.21203/rs.3.rs-646782/v1

Version of Record: A version of this preprint was published at Discover Materials on August 9th, 2021.
See the published version at https://doi.org/10.1007/s43939-021-00016-w.

Abstract

This article aims to study $MoSe_2$/CIGS tandem solar cells employing *SCAPS-1D* computational package based on ant colony algorithm. The simulation of Monolithic $MoSe_2$/CIGS tandem solar cells has been implemented successfully by employing the Matlab/Simulink. The power output of the Monolithic $MoSe_2$/CIGS tandem modules increases by the solar irradiations during the first few days of operation. The J-V characteristic and average daily energy production throughout the year has been calculated. The results show 80.71 % FF and 19.29 % efficiency of the solar cell. The other parameter for the ZnO/ZnS/$MoSe_2$ solar cell are V_{oc} = 0.62 V; J_{sc} = 38.69 mA/cm^2.

1. Introduction

There are many sources of renewable energy and solar energy is one of the most abundant of the sources [1, 2]. To harness the solar energy, solar radiations are directly converted into electrical energy by using photovoltaic cell which works on the photovoltaic effect [3]. There are many different variations of solar cells and the most common among them are the cells based on silicon for being cost effective [4, 5] and this has resulted in widespread usage of these solar cells in variety of applications [6–9]. The preparation of materials and fabrication of the solar cells with many layers of different materials is costly and time intensive. To investigate the material performance in complex systems, computational techniques, numerical method or simulations can be employed. In the present study also, the simulation technique has been applied to determine the variation of the properties critical for the performance of the solar cells. There are lots of experimental [10–12], theoretical [13–15] as well as computational studies [16, 17] about the potential materials that can be used in photovoltaic (PV) solar cells. Availability of computers with high computational powers and many computational packages, it has become relatively easy to carry out simulations prior to any experiment. In the present study, the computational study has been undertaken to determine the electrical energy generated by a $MoSe_2$/CIGS tandem solar cell. The electrical energy has been simulated with the variation of amount of solar energy received and optimum angle for orientation of the solar panels placed in Batna, Algeria located at 35.56° north, 6.19° east [18-20]. This summers in this desert area are longer & with higher temperatures during most of the year. Whereas winters are brief, warm with scarce rainfall. The optimum angle of orientation of the photovoltaic generator is kept between l to 32° with respect to the horizontal. The azimuth of 0° to the south, has been kept throughout the measurement [21, 22].

2. Material Parameters

Figure 1 presents the schematic diagram of the solar cell studied. The schematic diagram shows that the front contacts (exposed to light) on the left side, and the rear contacts on the right as simulated by SCAPS-1D convention. According to Shockley-Read-Hall (SRH) interface approach, the carriers from the conduction bands (CB) as well as valence bands (VB) can contribute in the interface recombination process.

Figure 1 describes different layers of the materials used in a PV device and the conventions. The following parameters are employed in this study: solar spectrum AM1.5, P = 100 mW/cm^2, and T = 300 K. Details of Materials parameters used in SCAPS-1D simulation are given in table 1.

Table 1: Materials Parameters used in solar cell simulation

Parameters	ZnO	SnS	$MoSe_2$	SnS	CIGS
Thickness (μm)	0.08	0.1	1	0.1	1
Eg (eV)	3.4	1.25	1.6	1.25	1.2
N_a (cm^{-3})	10^{14}	10^{14}	10^{14}	10^{14}	10^{14}
N_d (cm^{-3})	10^{20}	10^{20}	10^{6}	10^{20}	10^{6}

3. Ant Colony Optimization Algorithm

There are many probabilistic algorithms used to get the global optimal solution for all nonlinear problems and ant colony optimization (ACO) is one of these. . The ACO was implemented in different studies [23, 24], has been formulated to operate continuously, and can be easily adjusted to changing in environmental conditions. The main benefit of ACO's is its need of only one combination of voltage and current sensors that increases the system's reliability at considerably lower cost. This also increases the PV system's efficiency even though it is not applied to the distributed MPPT controllers. It has a set of associated parameters with graph components (either nodes or edges) and values of the components can be modified at runtime by the ants. The block diagram of the proposed system is shown in Figure 2.

The probability of an ant to move from node *i* to *j* is given below:

$$P_{ij} = \frac{T_{ij}^{\alpha}\eta_{ij}^{\beta}}{\sum T_{ij}^{\alpha}\eta_{ij}^{\beta}}$$

Whereas:

T_{ij}: is the amount of pheromone on edge *i, j*,,

α : a parameter to control the influence of T_{ij},

η_{ij}: is the desirability of edge *i j* (typically 1/dij),

β : is a parameter to control the influence of η_{ij}.

The variation in amount of pheromone is recorded using the following equation:

$$T_{ij} = \rho.T_{ij}(t-1) + \Delta T_{ij} \;/\; t = 1, 2, 3...T$$

ρ : Pheromone concentration rate (0-1).

ΔT_{ij} : is the amount of pheromone deposited.

4. Results And Discussion

Figure 3 presents the calculated (J-V) characteristic by simulation of $MoSe_2$ based solar cells having illumination below AM1.5 (100 mW/cm^2) and T = 300 K. At this stage the optimum thickness of $MoSe_2$ layer was set to 0.4 µm. From the model simulations, the (J-V) curve predicts short-circuit current densities (Jsc) and open-circuit voltages (Voc) as 38.69 mA/cm^2 and 0.62 V respectively.

The parameters of the cells deduced from the characteristic (J-V) plot are summarized in the Table 2.

Table 2
Photovoltaic parameters of ZnO/ZnS/$MoSe_2$

Solar cell configuration	
V_{oc} (Volt)	0.62
J_{sc} (mA/cm^2)	38.69
FF (%)	80.71
□ (%)	19.29
V_{MPP} (Volt)	0.53
J_{MPP} (mA/cm^2)	36.61

Figure 4 exhibits the amount of global radiations received per unit area of the system by the PV modules through a year. The irradiations start increasing from March and the estimated irradiations reach to the maximum (more than 327 kW/m^2) during July. The average daily energy production throughout the year is presented in Fig. 5. The energy production mirrors the global irradiations received. The energy production also increases with the increasing of received irradiations. The energy production increases with a peak in the month of July that is about 240 Wh/day and vice versa.

5. Conclusion

In this article, the simulation of Monolithic $MoSe_2$/CIGS tandem solar cells has been implemented successfully by employing the Matlab/Simulink. The power output of the Monolithic $MoSe_2$/CIGS tandem modules increases by getting exposure to light during the first few days of operation. The heat affects the solar panels Therefore; the yields of Monolithic $MoSe_2$/CIGS tandem are high even in desert environments.

Declarations

Acknowledgements

We gratefully acknowledge to Dr. Marc Burgelman, University of Ghent, Belgium, for providing the SCAPS-1D simulation software.

References

1. Zaynabidinov S, Aliev R, Muydinova M, Urmanov B. Appl Solar Energy. 2018;54:395.
2. Zaidi B, Saouane I, Shekhar C. Electrical Energy Generated by Amorphous Silicon Solar Panels. Silicon. 2018;10:975.
3. Martíneza O, Mass J, Tejero A, Moralejo B, Hortelano V. M.A. González.
4. Jiménez J, Parra V. Residual Strain and Electrical Activity of Defects.
5. in Multicrystalline Silicon Solar Cells. ACTA PHYSICA POLONICA A. 2014;125:1013.
6. Pudov AO, Kanevce A, Al-Thani H, Sites JR, Hasoon FS. Secondary barriers in CdS-CuIn1-xGaxSe2 solar cells. J Appl Phys. 2005;97:1063.
7. Zaidi B, Hadjoudja B, Chouial B, et al. Impact of hydrogen passivation on electrical properties of polysilicon thin films. Silicon. 2018;10:975.
8. Hao LZ, Gao W, Liu YJ, et al. High-Performance n-MoS2/i-SiO2/p-Si Heterojunction Solar Cells. Nanoscale. 2015;7:8304.
9. Yang C, Yin Y, Guo Y. Elemental selenium for electrochemical energystorage. J Phys Chem Lett. 2015;6:256.
10. Kautek W, Gerischer H. The photoelectrochemistry of the aqueousiodide/iodine redox system at N-type MoSe2 electrodes. Electro Chim. 1981;26:1771.
11. Wang G, Palleau E, Amand T, Tongay S, et al. Polarizationand time-resolved photoluminescence spectroscopy of excitons in MoSe2 monolayers. Appl Phys Lett. 2015;106:112101.
12. Jinlian Bi J, Ao L, Yao Y, Zhang G, Sun W, Liu F, Liu W, Li. Effect of Cu content in CIGSe absorber on MoSe2 formation during post-selenization process. Mater Sci Semicond Process. 2021;121:105275.
13. Mandati S, Misra P, Boosagulla D, Tata NR, Bulusu SV. Control over MoSe2 formation with vacuum-assisted selenization of one-step electrodeposited Cu-In-Ga-Se precursor layers. Environmental Science and Pollution Research 387; 2020.

14. Mavlonov A, Nishimura T, Chantana J, Kawano Y, Masuda T, Minemoto T. Back-contact barrier analysis to develop flexible and bifacial Cu(In,Ga)Se2 solar cells using transparent conductive In2O3: SnO2 thin films. Sol Energy. 2020;211:1311–7.
15. Rajagopal A, Yang Z, Jo SB, Braly IL, Liang PW, Hillhouse HW, Jen AK. Highly Efficient Perovskite-Perovskite Tandem Solar Cells Reaching 80% of the Theoretical Limit in Photovoltage. Adv Mater. 2017;29:1702140.
16. Kumar MH, Dharani S, Leong WL, Boix PP, Prabhakar RR, Baikie T, Shi C, Ding H, Ramesh R, Asta M, Graetzel M, Mhaisalkar SG, Mathews N. Lead-free halide perovskite solar cells with high photocurrents realized through vacancy modulation. Adv Mater. 2014;26:7122–7.
17. Green MA, Dunlop ED, Hohl-Ebinger J, Yoshita M, Kopidakis N, Hao X. Solar cell efficiency tables (version 56). Prog Photovoltaics. 2020;28:629–38.
18. Verschraegen J, Burgelman M. Numerical modeling of intra-band tunneling for heterojunction solar cells in SCAPS. Thin Solid Films. 2007;515:6276.
19. Zaidi B, Zouagri M, Merad S, Shekhar C, Hadjoudja B, Chouial B. Boosting Electrical Performance of CIGS solar cells: Buffer layer effect. Acta Phys Pol A. 2019;136:988–91.
20. Decock K, Khelifi S, Burgelman M. Modelling multivalent defects in thin film solar cells. Thin Solid Films. 2011;519:7481.
21. Burgelman M, Nollet P, Degrave S. Modelling Polycrystalline Semiconductor Solar Cells. Thin Solid Films. 2000;361:527.
22. Burgelman M, Verschraegen J, Degrave S, et al. Modeling thin-film PV devices. Prog Photovoltaics Res Appl. 2004;12:143.
23. Schlüter T. "Geological Atlas of Africa". Springer; 2008.
24. Ham A, Luckham N, Sattin A, "Algeria", Lonely Planet. (2007).
25. Jiang LL, Maskell DL, Patra JC. Energy Build. 2013;58:227.
26. Besheer A, Adly M, Industrial Technology (ICIT) 2012, IEEE International Conference on, 693 (2012).
27. Zaidi B, Belghit S, Shekhar C, Mekhalfa M, Hadjoudja B, Chouial B. Electrical Performance of CuInSe2 solar panels Using Ant Colony Optimization Algorithm. Journal of Nano- Electronic Physics. 2018;10:05045(pp3).

Figures

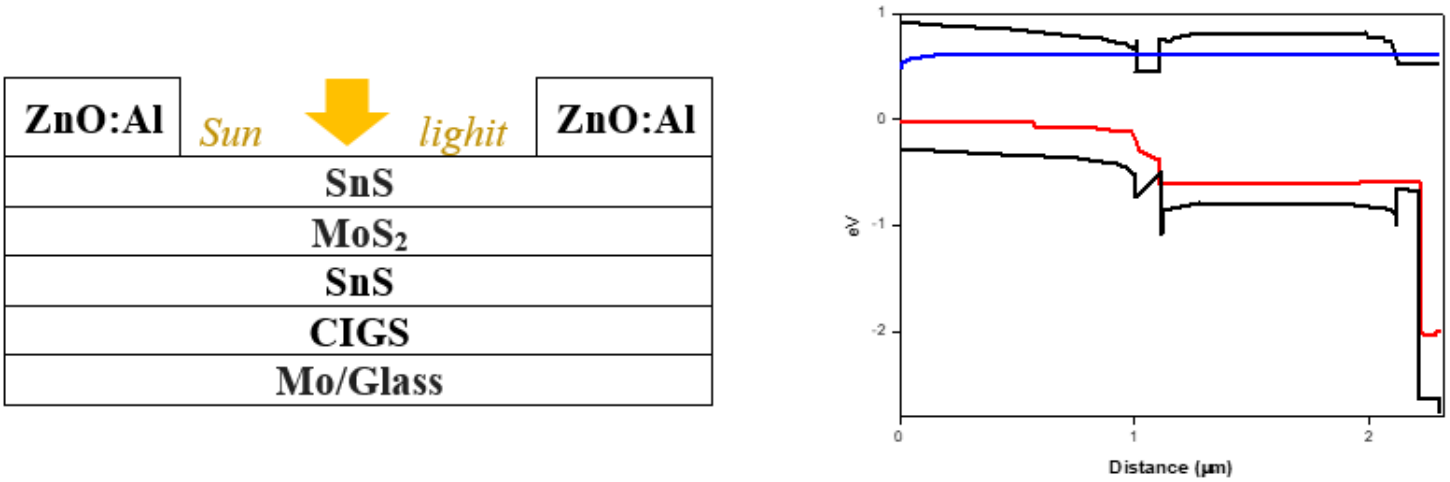

Figure 1

Structure (Left) and the energy band diagram (right) of the solar cell simulated by using SCAPS-1D

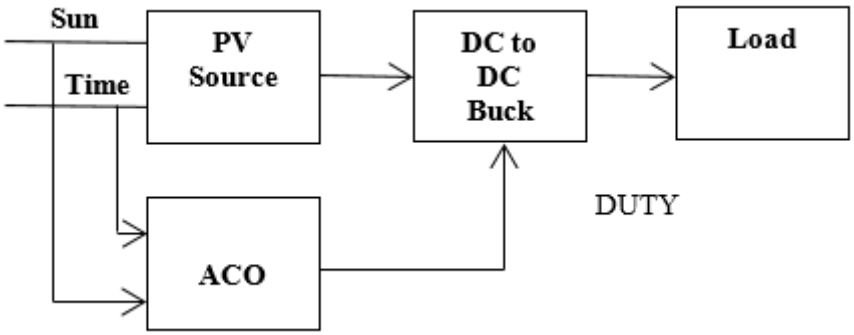

Figure 2

Block diagram of the proposed system [25]

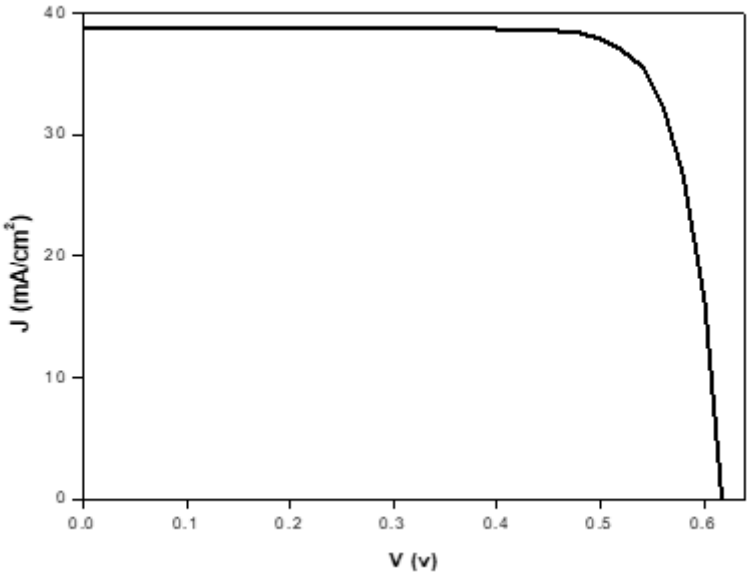

Figure 3

J-V characteristics of MoSe2 solar cells

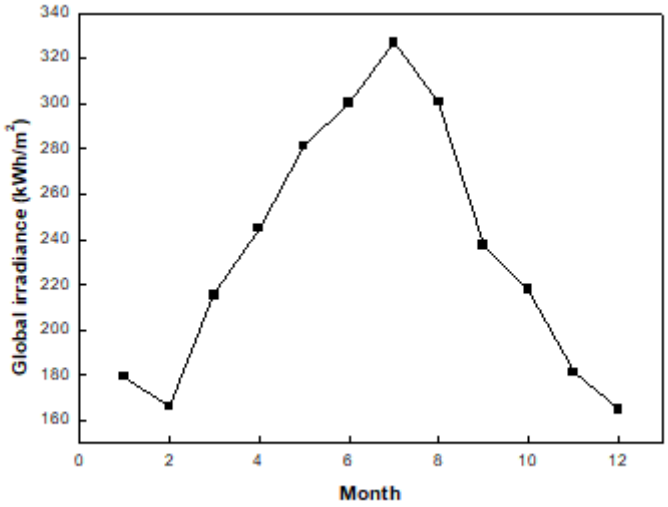

Figure 4

Estimation of global irradiance gathered by the modules solar cell

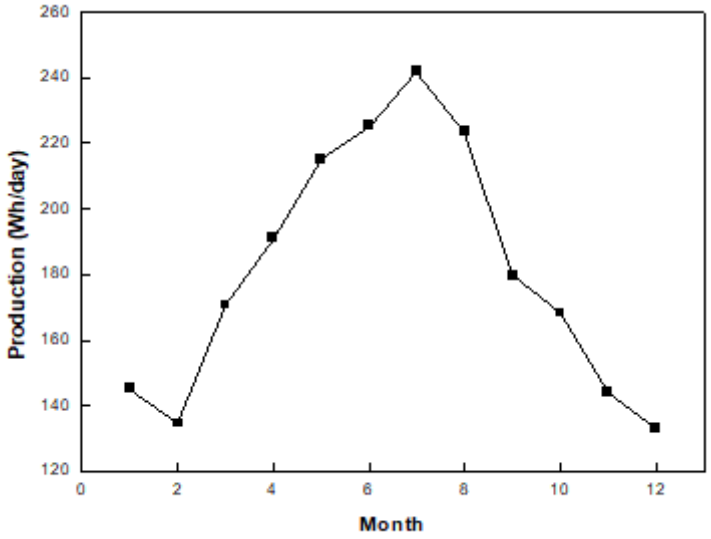

Figure 5

Average daily energy production throughout the year